Rapamycin Enhances CAR-T Control of HIV Replication and Reservoir Elimination in vivo
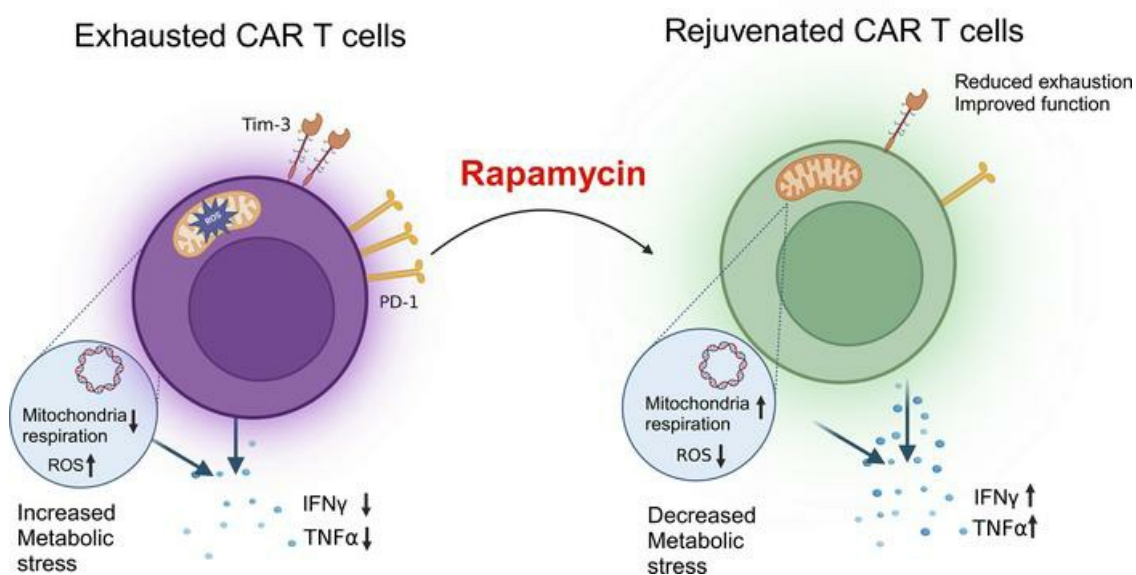
Wenli Mu, … , Scott D. Kitchen, Anjie Zhen

Research | In-Press Preview | AIDS/HIV | Immunology

Graphical abstract

1

Rapamycin Enhances CAR-T Control of HIV Replication and Reservoir Elimination *in vivo.*

3

Authors: Wenli Mu[1,2], Shallu Tomer[1,2], Jeffrey Harding[1,2], Nandita Kedia[1,2], Valerie Rezek[1,2], Ethan Cook[1,2], Vaibahavi Patankar[1,2], Mayra Carrillo[1,2], Heather Martin[1,2], Hwee Ng[1,2], Li Wang[1,2], Matthew D. Marsden[3,4], Scott G. Kitchen[1,2], and Anjie Zhen[1,2]*,

Affiliations:

[1]Division of Hematology/Oncology, Department of Medicine, David Geffen School of Medicine at UCLA, Los Angeles, CA, USA

[2]UCLA AIDS Institute and the Eli and Edythe Broad Center of Regenerative Medicine and Stem Cell Research, David Geffen School of Medicine at UCLA, Los Angeles, CA, USA,

[3]Department of Microbiology & Molecular Genetics, School of Medicine, University of California Irvine, Irvine, CA, USA

[4]Department of Medicine (Division of Infectious Diseases), School of Medicine, University of California Irvine, Irvine, CA, USA

*Correspondence to Anjie Zhen, BSRB 188, 615 Charles East Young Dr. South, Los Angeles, CA, 90095. Phone: 310.206.9719; Email: azhen@mednet.ucla.edu.

Conflict of interest: SK is cofounder of CDR3 therapeutics.

19

20

ABSTRACT

Chimeric Antigen Receptor (CAR) T cell therapy shows promise for various diseases. Our studies in humanized mice and non-human primates (NHPs) demonstrate that hematopoietic stem cell (HSCs) modified with anti-HIV CAR achieve lifelong engraftment, providing functional anti-viral CAR-T cells that reduce viral rebound after ART withdrawal. However, T cell exhaustion due to chronic immune activation remains a key obstacle for sustained CAR-T efficacy, necessitating additional measures to achieve functional cure. We recently showed that low dose rapamycin treatment reduced inflammation and improved anti-HIV T cell function in HIV-infected humanized mice. Here, we report that rapamycin improved CAR-T cell function both *in vitro* and *in vivo*. *In vitro* treatment with rapamycin enhanced CAR-T cell mitochondria respiration and cytotoxicity. *In vivo* treatment with low-dose rapamycin in HIV-infected, CAR-HSC mice decreased chronic inflammation, prevented exhaustion of CAR-T cells and improved CAR-T control of viral replication. RNAseq analysis of CAR-T cells from humanized mice showed that rapamycin downregulated multiple checkpoint inhibitors and the upregulated key survival genes. Mice treated with CAR-HSCs and rapamycin had delayed viral rebound post-ART and reduced HIV reservoir compared to CAR-HSCs alone. These findings suggest that HSCs-based anti-HIV CAR-T combined with rapamycin treatment is a promising approach for treating persistent inflammation and improving immune control of HIV replication.

INTRODUCTION

Engineering T cells with anti-HIV chimeric antigen receptors (CAR) has emerged as a promising gene therapy strategy to control HIV infection. HIV-specific CD8+ cytotoxic T lymphocytes (CTLs) are essential in suppressing HIV replication and eliminating HIV infected cells (1, 2). However, due to immune evasion by HIV (3) and development of dysfunctional HIV-specific T cells, natural CTLs are incapable of complete control of HIV replication in the absence of combination anti-retroviral therapy (ART) (4) and cannot eliminate reservoirs with "kick-and-kill" HIV cure strategies (5). A promising approach to overcome these barriers is through chimeric antigen receptor (CAR) engineered T cell therapy (6). T cells engineered with CD4-based CARs, which utilize CD4 extracellular domains to recognize HIV-1 Env, can effectively kill HIV infected cells and limit viral escape, as an escape from CD4 recognition would directly decrease viral fitness (7, 8). However, persistence, trafficking, and maintenance of function remain major challenges for peripheral CAR-T cell therapy (9). To overcome these issues, we showed that CAR modified hematopoietic stem cells (HSCs) are capable of lifelong engraftment and allow development of functional CAR-T cells *in vivo (10-12)*. Our studies in humanized mice (10, 11) and non-human primates (NHPs) (12, 13) demonstrated the feasibility and efficacy of the CAR-HSC therapy and showed that CAR-HSCs transplanted animals have reduced viral rebound after ART withdrawal. We have also made substantial improvements to this therapy by modifying the original CD4CAR construct to a second-generation CAR: termed D1D2CAR41BB. We showed that D1D2CAR41BB-HSC transplanted animals have improved CAR-T cell differentiation, better CAR-T cell persistence, and enhanced viral control (10). However, our lead CAR-HSC therapy still fell short of achieving complete viral remission in the absence of ART.

T cell exhaustion remains a major challenge for CAR T therapy for HIV-1 cure. Driven by chronic immune activation, T cell exhaustion remains one major barrier to achieving sustained immune surveillance for viral infection and cancer (14). Despite our recent successes in HSC-based CAR therapy, we found that HSCs-derived D1D2CAR41BB T cells are also subject to becoming exhausted. Similar CAR T cell exhaustion was also observed during peripheral anti-HIV CD4CAR T cell therapy in NHP models (15, 16).

64 Although antibodies targeting ICBs (immune checkpoint blockades, such as PD-1 blockade) may restore

65 CAR T cell function transiently (16, 17), ICB treatment can lead to serious side effects such as onset of

66 type 1 diabetes, colitis, and other adverse effects (18, 19) that may be unacceptable to ART treated HIV+

67 individuals. Therefore, alternative strategies to safely reverse or prevent CAR-T cell exhaustion are critical

68 for achieving long-term control of HIV replication.

69   Rapamycin, which inhibits mammalian Target of Rapamycin (mTOR) Complex 1, was first

70 approved for use in anti-cancer therapies and transplant rejection prevention. In recent years, rapamycin

71 has shown robust geroprotective ability, extending life spans in multiple model organisms, including the

72 life span of genetically heterogeneous mice from multiple research groups (reviewed in (20)). In humans,

73 rapamycin administration has been shown to reverse immunosenescence and boost response to seasonal flu

74 vaccines (21, 22) and it is being studied in multiple clinical trials in healthy individuals and individuals

75 with age-related diseases (23-25). Importantly, rapamycin can lead to metabolic reprogramming in T cells,

76 shifting metabolism from glycolysis to oxidative phosphorylation (OXPHOS) and modulating lipid

77 metabolism to enhance CD8 T cell memory formation (26, 27). While chronic treatment of humans with

78 high doses of rapamycin or analogs is associated with deleterious metabolic effects, recent studies in

79 humans have shown that a lower or intermittent dosing regimen of mTOR inhibitors in older adults is well

80 tolerated and leads to improved immune function and reduced infection in the elderly (21, 22, 28). A recent

81 study also demonstrated that rapamycin treatment during the beginning of chronic infection improves CD8

82 T cell memory formation and the efficacy of PD-1 targeted therapy (29). Moreover, our recent work showed

83 that intermittent *in vivo* treatment of HIV+ humanized mice with rapamycin led to reductions in immune

84 activation and improved endogenous anti-HIV T cell function, resulting in accelerated viral suppression

85 during ART and reduced viral rebound after ART withdrawal (30). Here we show that low dose, intermittent

86 rapamycin restores and improves anti-HIV CAR-T cell function during chronic HIV infection**.** We found

87 that rapamycin treatment notably remodeled the CAR-T cell transcriptome and improved mitochondria

88 function, resulting in enhanced anti-viral activities of CAR-T cells. This led to delayed viral rebound after

89 ART withdrawal and improved viral control by CAR-T cells, suggesting potential therapeutic values of

90 rapamycin in improving CAR-T cell function *in vivo*.

91

92 **RESULTS**

93 **Rapamycin treatment normalized anti-HIV CAR-T mitochondria metabolism and improved CAR-**

94 **T function *in vitro*.**

95 To examine if rapamycin modifies CAR T cell metabolism and restores exhausted anti-HIV-1 T

96 cell functions *in vitro*, we investigated the effects of rapamycin on D1D2CAR41BB modified primary T

97 cells that can recognize and kill HIV infected cells as described previously (10-12). CAR T cells were

98 generated by activating primary PBMCs from HIV seronegative individuals and transducing them with a

99 CAR expressing lentiviral vector. Afterward, CAR T cells were cultured *in vitro* for 2 weeks with IL-2 to

100 stimulate T cell proliferation and induce T cell exhaustion. After culture, cells were treated with either

101 rapamycin or vehicle control for 2 days followed by mitochondrial respiration analysis using a Seahorse

102 assay. As shown in **Fig. 1A**, oxygen consumption rates (OCR) over time were measured in the presence of

103 metabolic inhibitors to assess the impact of rapamycin treatment on mitochondrial function in CAR-T cells.

104 Basal OCR reflects oxygen consumption at rest (0-20mins), while maximal OCR measures capacity after

105 uncoupling the electron transport chain, allowing the mitochondria to operate at their maximal capacity

106 without generating ATP (40-70mins). Rapamycin-treated CAR-T cells demonstrated improved both basal

107 (**Fig. 1B**) and maximal mitochondria respiration levels (**Fig. 1C**), highlighting its potential ability to rescue

108 ATP-linked mitochondrial respiration in antiviral CAR-T cells. Rapamycin-treated CAR-T cells also

109 showed a reduction in mitochondria reactive oxygen species (ROS) by MitoSOX staining (**Fig. 1D**). These

110 results suggest that rapamycin can reduce ROS and enhance mitochondria functions in exhausted anti-HIV

111 CAR T cells. To investigate if rapamycin has a restorative effect on anti-HIV-1 CAR T cell function, we

112 tested rapamycin-treated CAR T cells' ability to produce pro-inflammatory cytokines and cytotoxic

113 capacity by co-incubating CAR T cells with control or target cells that express HIV envelope. As shown in

Fig. 1E and **Fig.1F**, we observed significant increases in both IL-2 and IFNγ production and improved cytotoxic killing activity by CAR T cells treated with rapamycin. Taken together, these data strongly suggest that rapamycin treatment can remodel anti-HIV CAR-T cell metabolism and restore anti-viral T cell function *in vitro*.

HIV induced HIV-specific CAR T exhaustion and dysfunction, while rapamycin treatment alleviated exhaustion and restored the viral suppression function of CAR T cells.

Driven by chronic antigen stimulation and persistent immune activation, T cell exhaustion remains one major barrier to achieving sustained immune surveillance for chronic viral infection (31, 32). Similarly, CAR-T cell exhaustion is observed during peripheral anti-HIV CAR T cell therapy in both humanized mice (15) and NHP models (16), undermining the efficacy of CAR-T therapy. Despite our recent successes in inhibiting HIV replication in humanized mice and NHPs using HSCs-based CAR therapy (10-12) and improved CAR-T cell memory formation with a second generation CAR containing the 41BB domain (10), viral loads rebounded in all CAR-HSCs transplanted animals after ART removal. Therefore, it is crucial to investigate immune exhaustion of HSC-derived CAR T cells in chronic HIV infection *in vivo*. Hence, we constructed humanized bone marrow-liver-thymus (BLT) NSG mice with HSCs mock transduced or transduced with lentiviral vectors expressing D1D2CAR41BB, as described previously (10). After immune reconstitution, we infected BLT mice with a high dose of HIV-1$_{NFNSXL9}$ (500ng of p24) to drive high viral loads and faster immune exhaustion (schematically shown in **Fig. 2A**). As expected, we observed a significant and gradual increase in the activation markers HLA-DR (**Fig. 2B**) and CD38 (**Fig. 2C**) on CAR T cells from peripheral blood after HIV infection (Representative flow gating strategy is shown in **SFigure1**). 3 weeks post infection, we also observed a significant increase in the exhaustion markers PD-1 and Tim-3 among CAR T cells (**Fig 2D-E)**. Consequently, while CAR mice demonstrated lower viral loads compared to mock 1 week after HIV infection, the viral suppression effects were lost by 3 weeks (**Fig 2F**), suggesting exhaustion/dysfunction of CAR T cells.

138   We previously demonstrated that low-dose and intermittent rapamycin treatment decreases chronic

139   inflammation and improves anti-viral T cell functions in HIV infected humanized mice (30). To further

140   evaluate whether rapamycin treatment alleviates HSCs derived CAR T exhaustion and restores control over

141   viral replication, we treated HIV infected mice with either rapamycin or vehicle for two weeks at 0.5mg/kg,

142   3 days a week as described in (30). Compared to vehicle-treated mice, we observed a significant decrease

143   in the activation markers HLA-DR and CD38, and exhaustion markers PD-1 and Tim-3, among CAR T

144   cells in the peripheral blood (**Fig. 2G**). Most importantly, we observed lower viral loads in rapamycin-

145   treated CAR mice compared to either mock or vehicle-treated CAR mice (**Fig. 2H**). Taken together, our

146   data suggest that rapamycin treatment alleviates CAR T exhaustion and potentially restores the anti-viral

147   functions of CAR T cells.

148   **Transcriptomic changes of CAR-T cells following rapamycin treatment in HIV infected humanized**

149   **mice.**

150   It is evident that rapamycin treatment changes the metabolic and functional activities of T cells *in*

151   *vivo*. To more closely examine the effects of rapamycin treatment and how it can affect the CAR-T cell

152   transcriptome, HIV infected HSCs-CAR humanized BLT mice were either treated with rapamycin or

153   vehicle for two weeks before necropsy. Afterward, splenocytes were isolated and CAR+ cells were sorted

154   (based on GFP expression), and bulk RNA sequencing was performed (schematically shown in **Fig.3A**). A

155   total of 0.5-1 million CAR (GFP+) cells were sorted as shown in **Fig. 3B** from each mouse. Principal

156   component analysis (PCA) showed that CAR cells derived from untreated mice clustered separately from

157   CAR cells isolated from rapamycin treated mice (**Fig. 3C**). Notably, as shown in **Fig. 3D**, the heatmap and

158   corresponding dendrogram clusters highlighted a downregulation of exhaustion-related markers, including

159   inhibitory receptors *PDCD1* (PD-1), *HAVCR2* (Tim3), *LAG3*, *SLAM7*, and exhaustion transcription factors

160   *EOMES* and *TOX* (33-38) in the rapamycin-treated CAR cells. Furthermore, rapamycin-induced a decrease

161   in type I interferon-related genes, such as *CXCL13* and interferon regulatory factors (*IRF)1* and *IRF4*, which

162   are known contributors to T-cell exhaustion (39-42). Corroborating our cytometric analysis (**Fig. 2G**), these

163   changes suggest that rapamycin mitigates T-cell exhaustion.

164   Intriguingly, rapamycin treatment also led to an upregulation of genes associated with T-cell

165   survival and persistence, notably those of the activator-protein-1 (AP-1) family, such as *JUN* and *FOS* (43-

166   45) as shown in **Fig. 3D**. As rapamycin is a potent autophagy inducer (30, 46), autophagy-related genes

167   such as *ATG13* and *ATG14* were also elevated post-treatment. Moreover, genes such as *IL2R*, *GZMA* and

168   *PRF1*, encoding IL2 receptor, granzyme A and perforin, respectively, which are crucial for the cytolytic

169   activity of T cells, displayed increased expression in the rapamycin-treated CAR cells (**Fig. 3D**). The box

170   plot visualization revealed notable differences in the log-normalized counts of key genes between the two

171   conditions as shown in **Fig.3E**.

172   We further investigated the gene expression involved in biological pathway signaling using KEGG

173   pathway analysis shown in **Fig. 3F**. Downstream targets of *MTOR*, including several cyclin-dependent

174   kinases (*CDKs*) that are involved in cell cycling pathways, were reduced. Concurrently, cell senescence

175   and apoptotic pathways were downregulated, as shown by lower *FAS* signaling and increased expression

176   of the anti-apoptotic gene *BCL2* in rapamycin-treated CAR T-cells (**Fig. 3F and Fig. 3E**). At the same

177   time, *NF-kB*, *JAK-STAT*, and *TNF* signaling pathways were upregulated in CAR T cells from rapamycin

178   treated mice. Collectively, these findings underscore rapamycin's comprehensive role in modulating CAR

179   T-cell function, effectively reducing exhaustion markers, and enhancing both survival and cytotoxic

180   capabilities.

181   **Low-dose rapamycin treatment in combination with ART reduced exhaustion of CAR T cells and**

182   **significantly reduced viral rebound.**

183   To further assess the effects of rapamycin treatment in combination with ART, we treated HIV

184   infected humanized mice transplanted with mock or CAR-modified HSCs with rapamycin or vehicle for 2

185   weeks, followed by 4 weeks of ART treatment and ART withdrawal (**Fig 4A**). As shown in **Fig. 4B,**

186   compared to control mice, ART combined with rapamycin significantly reduced the expression of immune

187   activation markers (HLA-DR, CD38), and exhaustion markers (PD-1, Tim3) among CAR-T cells in the

188   blood and spleen at necropsy. TOX is a key transcription factor that regulates the T cell exhaustion program

189   and the expression of TOX has been associated with cellular exhaustion during chronic infection (33, 35,

190   47). Similar to our RNAseq studies (**Fig 3D**), flow analysis of CAR-T cells at necropsy also showed

191   significant down regulation of TOX expression of CAR-T cells from mice treated with rapamycin as

192   compared to vehicle control (**Fig. 4C**).

193   To study the effects of rapamycin treatment on HIV suppression, persistence, and viral rebound in

194   CAR mice, plasma viral loads were measured longitudinally. As shown in **Fig. 4D**, at 9 weeks post-HIV

195   infection and after 4 weeks of ART, all mice exhibited full viral suppression with undetectable viral load.

196   One week after interrupting ART, all mock control and vehicle-treated CAR mice, and all but 2 rapamycin-

197   treated CAR mice experienced viral rebound. Three weeks after ART withdrawal, all mice showed viral

198   rebound. However, rapamycin-treated CAR mice maintained a significantly lower viral load as compared

199   to vehicle-treated CAR mice, or mock mice treated with either vehicle or rapamycin. Additionally, we

200   observed significantly lower levels of viral DNA (**Fig. 4E**) and cell associated HIV RNA (**Fig. 4F**) in the

201   blood, spleen, and bone marrow at necropsy after ART withdrawal, indicating a reduction in overall viral

202   burden in the rapamycin-treated CAR mice. Taken together, these data suggest that the combination of

203   rapamycin and ART treatment improves CAR T cell function- in HIV suppression and reduces viral

204   rebound.

205   **Rapamycin treatment reduced mitochondria ROS in CAR T cells and improved CAR T function.**

206   Excessive ROS can cause damage to cellular components, including lipids, proteins, and DNA (48,

207   49). Decreased mitochondrial biogenesis and excessive production of mitochondrial ROS can exacerbate

208   mitochondrial dysfunction and immune exhaustion in T cells (50-54). Our *in vitro* data suggested that

209   rapamycin treatment protects the mitochondria against oxidative stress in CAR T cells (**Fig 1D**). To further

210   investigate the potential for *in vivo* rapamycin treatment to reduce oxidative stress and alleviate

211   mitochondrial injuries in CAR T cells, we measured mitochondrial dysfunction levels using MitoSOX to

212 detect mitochondrial superoxide levels in CAR T cells from both peripheral blood and spleen of CAR mice

213 treated with rapamycin or vehicle control. We observed that CAR T cells from mice treated with rapamycin

214 exhibited significantly lower mitochondrial ROS compared to vehicle-treated mice (**Fig. 5A**), suggesting a

215 reduction of oxidative stress in treated mice.

216   To further investigate whether HIV-specific CAR T cell responses were improved in the ART and

217 rapamycin combined-treatment group, splenocytes from rapamycin or vehicle treated mice were stimulated

218 with mitogens PMA/ionomycin, or stimulated with HIV target cells (stimulated latently infected ACH2

219 cells, which are Env+) or control cells (unstimulated ACH2 cells, which are Env-). Compared with the

220 vehicle-treated control, CAR T cells from rapamycin-treated infected mice produced significantly higher

221 levels of pro-inflammatory IFN-γ and TNF-α cytokines after PMA/ionomycin stimulation (**Figs. 5B, 5C**),

222 and HIV Env+ cells, indicating improved proinflammatory cytokine production and anti-viral responses of

223 CAR T cells. In summary, these data suggest that a combination of rapamycin and ART reduced ROS and

224 improved anti-HIV functions of CAR T cells *in vivo*.

225 **Short-term Rapamycin treatment in CAR-HSCs NSG-Tg (IL-15) humanized mice showed delayed**

226 **viral rebound and smaller reservoirs after ART withdraw**

227   An enhanced humanized mouse model, termed Hu-NSG-Tg(IL-15), which was engineered to express

228 physiological level of human IL-15, was reported to support more robust engraftment of human immune

229 cells, including T cells, B cells, and NK cells, and therefore represents a valuable model for studying HIV

230 pathogenesis and immune responses (55, 56). We adopted this new model to make HSCs-CAR mice and

231 examined the effects of rapamycin or vehicle treatment. Importantly, to examine if the effects of rapamycin

232 treatment persist after short-term treatment, rapamycin treatment was started with ART and stopped 2

233 weeks after ART withdrawal, and mice were continuously monitored for an additional 3 weeks before

234 necropsy (shown in **Fig 6A**). As shown in **Fig. 6B,** two weeks after ART interruption, viral loads quickly

235 rebounded in all mice (100%, 4/4) from the mock group. In CAR-HSCs vehicle-treated group, two out of

236 four did not rebound (50%, 2/4) 2 weeks after ART withdrawal. However, all mice rebounded 4 weeks after

237   ART interruption. In contrast, none of the rapamycin-treated CAR-HSCs mice had viral rebound 2 weeks

238   after ART. 2 weeks after cessation of rapamycin treatment and 4 weeks after ART cessation, three out of

239   six (50%) rapamycin CAR-HSCs mice did not rebound. 5 weeks after ART withdrawal at necropsy, two

240   out of six (33%) rapamycin-treated CAR-HSCs mice continued to have undetectable viral load, while the

241   other four maintained lower viral loads after rebound. In summary, we observed that rapamycin-treated

242   CAR mice had improved CAR suppression of viral replication, leading to delayed viral rebound after ART

243   cessation, as shown in **Fig 6C**. Importantly, As shown in **Fig 6D**, we observed an overall decrease in the

244   level of cell associated HIV DNA and RNA in the spleen and bone marrow in rapamycin-treated CAR mice

245   compared to vehicle-treated CAR mice, and mice with undetectable viral loads also showed

246   low/undetectable viral DNA/RNA in tissues, suggesting lower reservoir in rapamycin-treated CAR mice.

247

248   **DISCUSSION**

249   CAR redirected T cell immunity against HIV-1 represents a highly promising approach that can be

250   used in most HIV infected individuals. CARs recognize target cells through direct binding to specific cell

251   surface antigens and are HLA-unrestricted, bypassing a major limitation for T cell immunotherapies (57).

252   Now widely applied for cancer, some of the first CAR clinical trials were for HIV-1 infection (58-60). The

253   "original" HIV-specific CARs were composed of a CD4 extracellular domain linked to the intracellular

254   CD3-ζsignaling domain (CD4CAR), utilizing CD4 binding to HIV-1 Envelope (Env) for targeting and

255   killing of HIV-1-infected cells (8). HIV-1 envelope interaction with CD4 is critical for viral replication,

256   thus limiting viral escape from a CD4-based CAR (61). Tremendous progress has been made using CD4

257   based CAR T cell therapy against HIV infection since its invention. Improvement in the CAR design have

258   been made with modification of the Env recognition domain and inclusion of co-stimulatory domains, and

259   enhanced CD4-based CAR-T cell efficacy has been demonstrated by multiple groups of investigators (6,

260   15, 62-64), including ours (10, 12, 13, 65-68), and it is currently under investigation in multiple clinical

261   trials (ClinicalTrials.gov Identifier: NCT03617198, NCT04648046).

262

Given the challenge of HIV latent reservoirs driving chronic infection and persistence under suppressive ART, the functional persistence of CAR T cells is critical for successful long-term immune containment of HIV infection. HSCs based gene therapy supports lifelong generation of functional immune progeny, giving rise to a stable supply of gene-modified CAR T cells. We have shown that HSCs-based CAR therapy allows for lifelong, persistent production of functional CAR-T cells to control viral replication from reactivated reservoirs, and HSCs-based CAR therapy showed better persistence and trafficking to tissue reservoirs than periphery blood derived CAR T cells (10, 11, 13, 65, 67). Despite their *in vivo* efficacy in reducing viral replication and reservoir, HSCs-derived CAR-T cells cannot achieve full viral suppression after ART withdrawal. Persistent type I Interferon signaling and immune activation during chronic HIV infection are driving forces of immune dysfunction (69, 70), and engineered CAR-T cells are also subject to this immune exhaustion. Previously we demonstrated that targeting persistent type I interferon signaling, either by blocking type I interferon receptor (71), or inducing autophagy by rapamycin (30, 69, 72), can lead to reduced hyperinflammation and improved anti-HIV T cell function *in vivo*. In the current study, we found that rapamycin treatment also improved CAR-HSCs therapy in HIV infected humanized mice. Rapamycin treatment reduced persistent immune activation, rejuvenated CAR-T cell function, leading to delayed viral rebound and better viral control after ART cessation, even after rapamycin treatment was stopped. Notably, two out of six rapamycin treated CAR-HSCs continued to have undetectable viral loads five weeks after ART withdrawal and three weeks after rapamycin cessation, while all other groups had 100% viral rebound. The rapamycin treatment also led to reduced cell-associated HIV RNA and DNA in blood and multiple lymphoid tissues in CAR-HSCs mice. Importantly, we observed improved mitochondria function and substantial transcriptomic modification of CAR-T cells by rapamycin treatment, suggesting the dual beneficial effects of rapamycin in reducing T cell inhibitory receptors while simultaneously promoting stemness-related gene expression, offering promising insights into the optimization of CAR T-cell therapy for sustained anti-HIV responses.

287   Rapamycin is a mTOR inhibitor, which is a major regulator of cellular metabolism and the cellular

288   ageing process. First discovered and FDA-approved for treatment of various cancers and as an

289   immunosuppressant, rapamycin's effects on aging are increasingly recognized and used for longevity

290   studies (20, 73). Multiple studies suggest that rapamycin treatment extends health span and improves the

291   function of the aging immune system, such as improving antiviral activities in older adults (21, 22, 28).

292   This is of relevance to HIV, as people living with HIV are aging with greater life expectancy due to effective

293   ART. Despite the success of ART, the difference in comorbidity-free years between PLWH and the general

294   population persists, and premature immune aging has been shown to be the major culprit driving age-related

295   co-morbidity (74-76). A recent clinical study demonstrated that Sirolimus (rapamycin) reduced CD4+ T

296   cell cycling and PD-1 expression on CD8+ T cells in PLWH, underscoring its potential to impact HIV

297   reservoirs by modulating immune activation and exhaustion pathways (77). These findings align with our

298   observations in humanized mice and support previous findings where treatment with rapamycin was

299   correlated with reduced HIV reservoir in HIV-1 infected kidney transplant recipients (78). Rapamycin also

300   has documented antiviral properties through mTOR inhibition (79). To further delineate the dual

301   mechanisms of rapamycin—direct antiviral effects and immunomodulation (80)—additional studies such

302   as depleting CD8+ T cell responses could help clarify the role of rapamycin in modulating immune-

303   mediated clearance of infected cells versus its direct impact on viral replication. In addition, while our study

304   highlights the effects of rapamycin in enhancing CAR-T cell function, its potential to directly modulate

305   endogenous CTLs and other immune cell populations, such as NK cells, should also be considered.

306   Therefore, additional studies should be carried out to further explore the therapeutic effects of rapamycin

307   on different immune cell types. However, as a master regulator, mTOR signaling plays a key role in T cell

308   fate, such as effector versus memory differentiation, and its regulation needs to be tightly controlled (81).

309   Treatment with daily rapamycin can limit T cell proliferation in SIV infected rhesus macaques on

310   antiretroviral therapy and was not shown to impact SIV reservoir (82). For our current study, we chose to

311   use lower and intermittent dosing of rapamycin that we previously described, which did not impact T cell

312 homeostasis (30). Therefore, careful studies on the dosing and treatment regimen of rapamycin are needed

313 to maximize its effects and reducing its toxicity in animal models and in clinical studies.

314   In summary, our study describes the effects of rapamycin on improving the function of anti-HIV

315 CAR-T cells *in vivo*, demonstrating its impact on CAR-T cell metabolism and transcriptomic modification.

316 We believe that the results described in this study shed light on potential strategies to augment CAR-T

317 functions for treating HIV infection, and our findings may also be applicable to other CAR-T therapies that

318 are affected by immune exhaustions (83).

319

320

321 **MATERIALS AND METHODS**

322 **Sex as a biological variable.** Both male and female human PBMC or tissue donors and animals were

323 included in all experiments.

324 **Lentivirus production.**

325 The lentivirus-based D1D2CAR41BB vectors were produced in Lenti-X 293T cells (Takara Bio) using the

326 Lipofectamine 2000 reagent (Invitrogen). Briefly, Lenti-X 293T cells were co-transfected with

327 D1D2CAR41BB vector with pCMV.ΔR8.2.Δvpr packaging construct and the pCMV-VSV-G envelope

328 protein plasmid, as previously described (1, 2). The supernatant was obtained from transfected Lenti-X

329 293T cells 48 hours post-transfection. It underwent filtration using a 0.45 μm sterile filter and concentration

330 through ultracentrifugation using a Beckman SW32 rotor at 154,000g at 4°C. Following aspiration of the

331 medium, the pellet was resuspended in PBS and stored at –80°C.

332 **Transduction of CAR T cells.**

333 Primary T cells were sorted from primary PBMC from healthy donors using Pan T cell isolation kit – human

334 (Miltenyi Biotec, # 130-096-535). Isolated T cells were stimulated with plate-bound anti-CD3 and anti-

CD28 (Miltenyi Biotec) at 2 million cells/ml. After activation for at least 24 hrs, cells were washed and transduced with CD4CAR vector on retronectin-coated plate with cytokine IL-2. Cells were cultured in RPMI supplemented with 10% FBS and 1% Pen/strip with IL-2 for additional 2 weeks. Following this culture period, the cells were treated with either DMSO control or rapamycin at a concentration of 500pM for 2 days, prior to conducting the Seahorse assay.

Seahorse assay.

250,000 CAR-T cells were seeded into wells of a poly-d-lysine-coated (100 μg/mL) XF96 spheroid plate. Cells in the plate were centrifuged at 450 rpm for 7 min with no centrifuge brake, mitochondrial respiration was measured using the Seahorse XF96 extracellular flux analyzer equipped with a spheroid plate-compatible thermal tray (Agilent Technologies). Basal respiration was first measured in 3 mM glucose media. To validate cell respirometry with the XF96 spheroid plate, CAR-T cells were then sequentially exposed to glucose (final concentration in well of 20 mM), Oligomycin A (3.5–4.5 μM final concentration), FCCP (1 μM final concentration) and Antimycin A (Ant A, 2.5 μM final concentration).

Humanized mice generation.

D1D2CAR41BB BLT mice were constructed similarly to previously reported HIV-1 Triple CAR BLT humanized mice(68). Briefly, human fetal liver derived CD34+ cells were purified by immunomagnetic separation. Cells were then transduced overnight with D1D2CAR41BB lentiviruses with retronectin-coated plates. On day of transplant, NOD.Cg-PrkdcscidIl2rgtm1Wjl/SZJ (NOD/SCID/IL2Rγ−/− or NSG, The Jackson Laboratory) or NOD.Cg-Prkdcscid Il2rgtm1Wjl Tg(IL15)1Sz/SzJ (NSG-huIL15, The Jackson Laboratory) mice received 2.7 Gy total body sublethal irradiation and then were transplanted with transduced CD34+ in Matrigel (Corning Life Sciences), liver and thymus tissue under the kidney capsule, with tissue from the same donor as the CD34+ cells. Afterward, mice were injected with ∼0.5×10^6 lentivirus-based CAR vector transduced CD34+ cells. At 8–10 weeks post-transplantation, each mouse was bled retro-orbitally and peripheral blood mononuclear cells analyzed by flow cytometry to check human

359   immune cell engraftment. Upon stable human leukocyte reconstitution efficiency more than 50%, mice

360   were used for HIV-1 infection and further experiments.

361   **HIV-1 infection, ART and rapamycin treatment.**

362   The R5 tropic strain of HIV-1$_{NFNSXSL9}$ was generated by transfection of 293T cells with plasmid containing

363   full-length HIV-1$_{NFNSXSL9}$ genome. Humanized mice were infected with HIV-1$_{NFNSXSL9}$ (500 ng p24 per

364   mouse) through retro-orbital injection while under inhalant general anesthesia. Infected mice with

365   demonstrable viral infection were treated for 6 weeks with ART drugs. The ART regimen is consisted of

366   tenofovir disoproxil-fumarate (TDF, 80mg/kg), emtricitabine (FTC, 120mg/kg), and Elvitegravir

367   (ELV160mg/kg) given by food. TDF, FTC and ELV were generously supplied by Gilead Sciences. TDF,

368   FTC and ELV were dissolved in DMSO and mixed with sweetened moist gel meal (DietGel Boost,

369   ClearH2O; Medidrop Sucralose) as previously described (84). For rapamycin treatment, mice were injected

370   i.p. with 0.5 mg/kg rapamycin (LC laboratories) 3 times a week.

371   **Flow cytometry.**

372   Mitochondria-associated ROS levels were measured by staining cells with MitoSOX (Molecular

373   Probes/Invitrogen) at 5 μM for 40 min at 37 °C. Cells were then washed with PBS solution and resuspended

374   in PBS solution containing 2% FBS for FACS analysis. Single-cell suspensions prepared from peripheral

375   blood or spleen of humanized mice were stained using the following antibodies for flow cytometry: CD45

376   (Invitrogen, clone HI30), CD3 (Invitrogen, clone OKT3), CD4 (Invitrogen, clone RPA-T4), CD8

377   (Invitrogen, clone SK1), CD38 (Invitrogen, clone HIT2), HLA-DR (BD Bioscience, clone L240), CD45RA

378   (BD Bioscience, clone HI100), CD62L (Invitrogen, clone DREG-56), IFN-γ (BioLegend, clone 4S.B3),

379   IL-2 (BioLegend, clone MQ1-17H12), TNF-α (BioLegend, clone Mab11), Tox (Invitrogen, clone

380   TXRX10), PD-1 (Invitrogen, clone ebioJ105), and, TIM-3 (BioLegend, clone F38-2E2). LIVE/ DEAD

381   Fixable Yellow Dead Cell Stain Kit (Invitrogen) was used. Abs for cell surface markers and intracellular

382   markers were conjugated to FITC, phycoerythrin (PE), PerCP-Cy5.5, PE-Cy5, PE-Cy7, electron coupled

383   dye (ECD), allophycocyanin (APC), APC–eFluor780, Alexa Fluor 700, eFluor450, Pacific Orange, or

16

384 Pacific Blue in the appropriate combination. The LSRFortessa flow cytometer and FACSDiva software

385 (BD Biosciences) were employed to obtain the cells, while FlowJo software was used for data analysis. A

386 minimum of 1000 cells were acquired for each analysis, and each flow plot, representative of the data, was

387 replicated more than three times.

388 **Nucleic acid extraction and real time PCR.**

389 To measure HIV plasma viremia, viral RNA was extracted from plasma and 1-step real-time PCR was

390 performed using the TaqMan RNA-to-Ct 1-Step Kit (Thermo Fisher Scientific, USA) with the following

391 primers and probe:

392 HIV-1 forward primer: 5′-CAATGGCAGCAATTTCACCA-3′;

393 HIV-1 reverse primer: 5′-GAATGCCAAATTCCTGCTTGA-3′;

394 HIV-1 probe: 5′-[6-FAM] CCCACCAACAGGCGGCCTTAACTG [Tamra-Q]-3′;

395 To measure the levels of cell-associated HIV RNA with HPRT1 as an internal control, cells were harvested

396 for RNA extraction according to manufacturer's protocol (Qiagen) and making of cDNA using the High-

397 Capacity cDNA Reverse Transcription Kit (Thermo Fisher Scientific). For HPRT1, Single Tube TaqMan

398 Gene Expression Assays (Thermo Fisher Scientific) human HPRT1 (Hs01003267_m1) was used. Relative

399 mRNA expression was calculated by normalizing genes to HPRT1 mRNA expression.

400 To measure the levels of cell-integrated HIV DNA with RPP30 as an internal control, cells were harvested

401 for DNA extraction according to manufacturer's protocol (Qiagen). For HIV DNA as well as RPP30, Single

402 Tube TaqMan Gene Expression Assays (Thermo Fisher Scientific). Relative DNA integration was

403 calculated by normalizing HIV DNA to RPP30 gene count.

404 HIV-1 forward primer: 5′-CAATGGCAGCAATTTCACCA-3′;

405 HIV-1 reverse primer: 5′-GAATGCCAAATTCCTGCTTGA-3′;

406 HIV-1 probe: 5′-[6-FAM] CCCACCAACAGGCGGCCTTAACTG [Tamra-Q]-3′;

407   RPP30 Forward primer: 5′-GATTTGGACCTGCGAGCG-3′;

408   RPP30 Reverse primer: 5′-GCGGCTGTCTCCACAAGT-3′;

409   RPP30 Probe: /5HEX/TTCTGACCT/ZEN/GAAGGCTCTGCG/3IABkFQ/-3′

410   **D1D2CAR sorting and RNA sequencing.**

411   Spleens from D1D2CAR transduced mice were collected, mashed over a 70 μm cell strainer, and

412   resuspended into single cell suspensions in complete RPMI after red blood cell lysis using ACK lysis buffer

413   (Thermo Fisher). 0.5-1 million GFP+ single live cells were sorted using BD FACS Melody (BD

414   Biosciences) from splenocytes per mouse. Three replicates of each experiment were carried out. RNA

415   extraction was done using RNeasy kits (Qiagen). Sample QC and integrity (RIN-equivalent values) was

416   performed using Tapestation Analysis software v3.2, Agilent Technologies. Sequencing was carried out

417   using Illumina NovaSeq platform. Raw sequence data of different treatment conditions (in triplicate) were

418   pre-processed for quality using Fastqc. Trimmomatic was used for adaptors and quality trimming. After

419   this, reads were aligned onto human genome (hg38) using STAR aligner. SAMtools was used to convert

420   SAM files BAM files. Mapped reads were counted across human genes by using tool featureCounts (75)

421   that provided raw counts data by assigning mapped reads to genes. Differential gene expression analysis

422   with the raw read counts data using R package DESeq2. Raw sequence data and processed data have been

423   deposited to GEO. Gene expression data was analyzed using Gene Set Enrichment Analysis (GSEA)

424   software tool. For pathway analysis, STRING (Search Tool for the Retrieval of Interacting Genes/Proteins)

425   software was used.

426   **Statistics.**

427   A total of 2 independent cohorts of mice (n = 15–30 total mice, each constructed from the same donor

428   tissues) were used in this study for various experiments. Two cohorts were pooled for comparing between

429   groups. All statistical analyses were performed using Prism 9.0 software (GraphPad) or R software v4.3.1.

430   To compare statistical difference between 2 groups, Mann-Whitney U tests were used. For analysis of data

431 that contains more than 2 groups (depicted in Figure 2B-E, Figure 2H, Figure 4D, Figure 4E and Figure

432 4F), the Kruskal-Wallis test was performed to compare samples; and all of these data have *P* values less

433 than 0.05 by Kruskal-Wallis or Mann-Whitney were considered statistically significant. Exact statistical

434 tests are also reported in figure captions.

435 **Study approval.**

436 Peripheral blood mononuclear cells were obtained at UCLA in accordance with UCLA IRB–approved

437 protocols under written informed consent using an IRB-approved written consent form by the UCLA Center

438 for AIDS Research Virology Laboratory and distributed for this study without personal identifying

439 information. Human fetal tissue was purchased from Advanced Biosciences Resources or Cercle Allocation

440 Services and was obtained without identifying information and did not require IRB approval for its use.

441 Animal research described in this article was performed under the written approval of the UCLA Animal

442 Research Committee in accordance with all federal, state, and local guidelines. All surgeries were

443 performed under ketamine/xylazine and isoflurane anesthesia, and all efforts were made to minimize animal

444 pain and discomfort.

445 **Data and code availability.**

446 Raw data are in the Supporting Data Values file. RNA-Seq data generated in this study have been deposited

447 in the NCBI's Gene Expression Omnibus (GEO) database (GEO GSE 284491). No original code is

448 reported. All other raw data and materials are available from the corresponding author upon request.
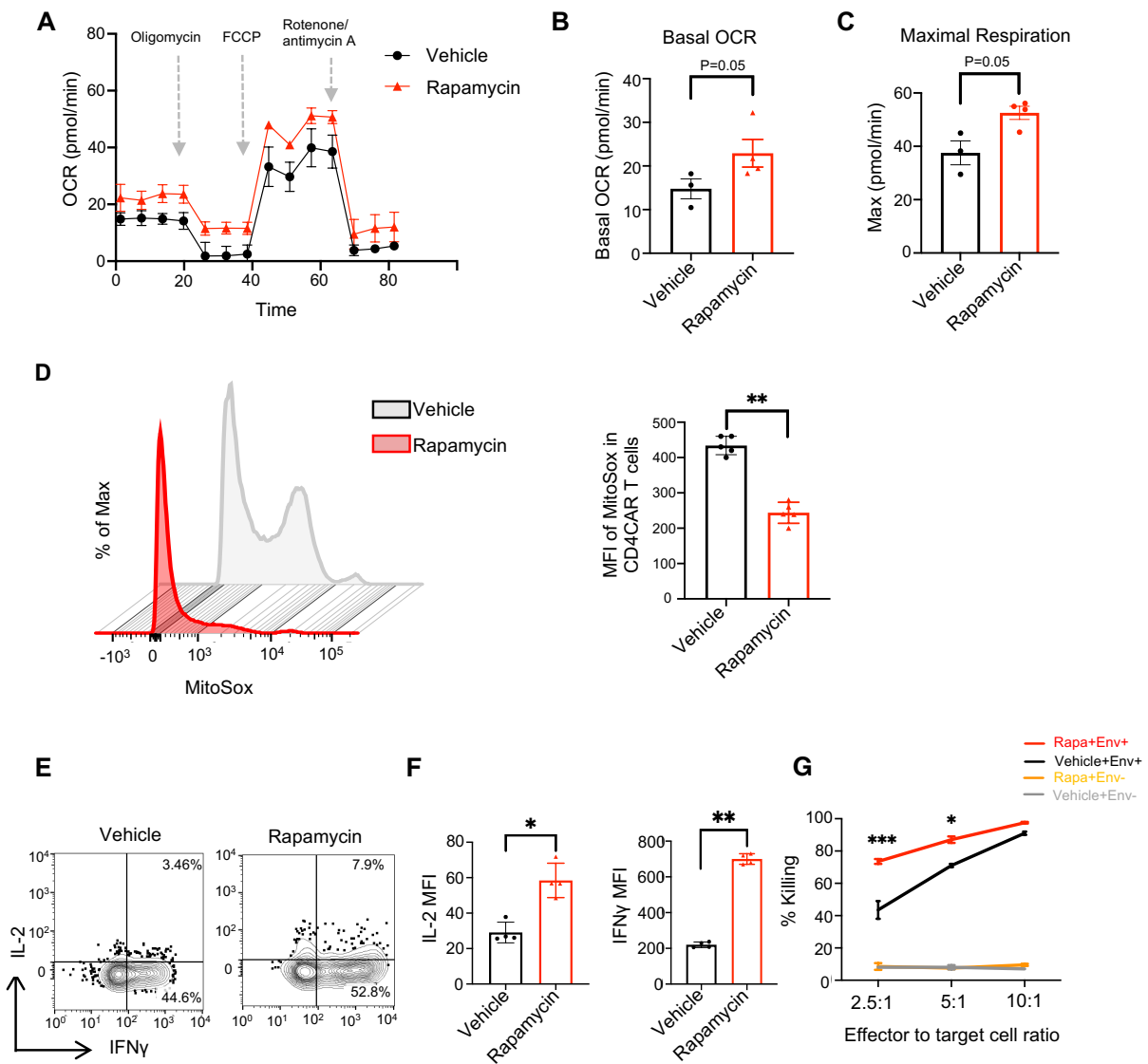
449

464

**Author contribution:**

466   WM and AZ designed the experiments. WM, ST, JH, NK, VR, EC, VP, MAC, HM, HG and LW conducted

467   the experiments. WM, JH, ST, NK and AZ analyzed the data. WM and AZ wrote the original draft, JH, ST,

468   NK, HM, MDM and SGK reviewed and edited the manuscript.

469

470

Figure and Figure legend

Figure 1. Treatment of anti-HIV CAR-T cells with rapamycin modified cellular metabolism *in vitro*. anti-HIV CD4CAR-T cells were produced by transducing activated primary PBMCs from healthy donors. Cells were then sorted to >90% CAR+ purity and expanded using 100IU/ml IL-2 for 2 weeks to promote exhaustion, followed by treatment with either DMSO, or 50pM of Rapamycin for 2 days. Afterwards, seahorse assay was performed on treated CAR T cells. **A**) The oxygen consumption rates (OCRs) over time changes under basal metabolic conditions and in responses to metabolic inhibitors. **B**) Basal OCR levels. **C**) Maximal respiratory levels. **D**) ROS were analyzed in CD4CAR-T cells labeled with MitoSOX after treatment as shown by flow cytometry and MFI summary of MitoSox. **E-F**) Cytokine assay. Vehicle or rapamycin treated CAR-T cells were cocultured with HIV Env expressing (stimulated ACH2) cells overnight, followed by Golgiplug for 6 hours. Percentage of IFN-γ and IL-2 expression were measured by flow cytometry in CD4CAR-T cells. Representative flow plot and summary was shown in E and F. **G**) Killing assay. Vehicle or rapamycin treated CAR-T cells were cocultured with either HIV Env+ (stimulated ACH2) or HIV Env- (unstimulated ACH2) cells overnight at 2.5:1, 5:1 and 10:1 ratio. Specific killing activity is shown for vehicle treated and rapamycin treated CAR-T cells. All values are means ± SD of at least three independent experiments. Mann-Whitney test (unpaired); *$P < 0.05$, **$P < 0.01$, ***$P < 0.001$.
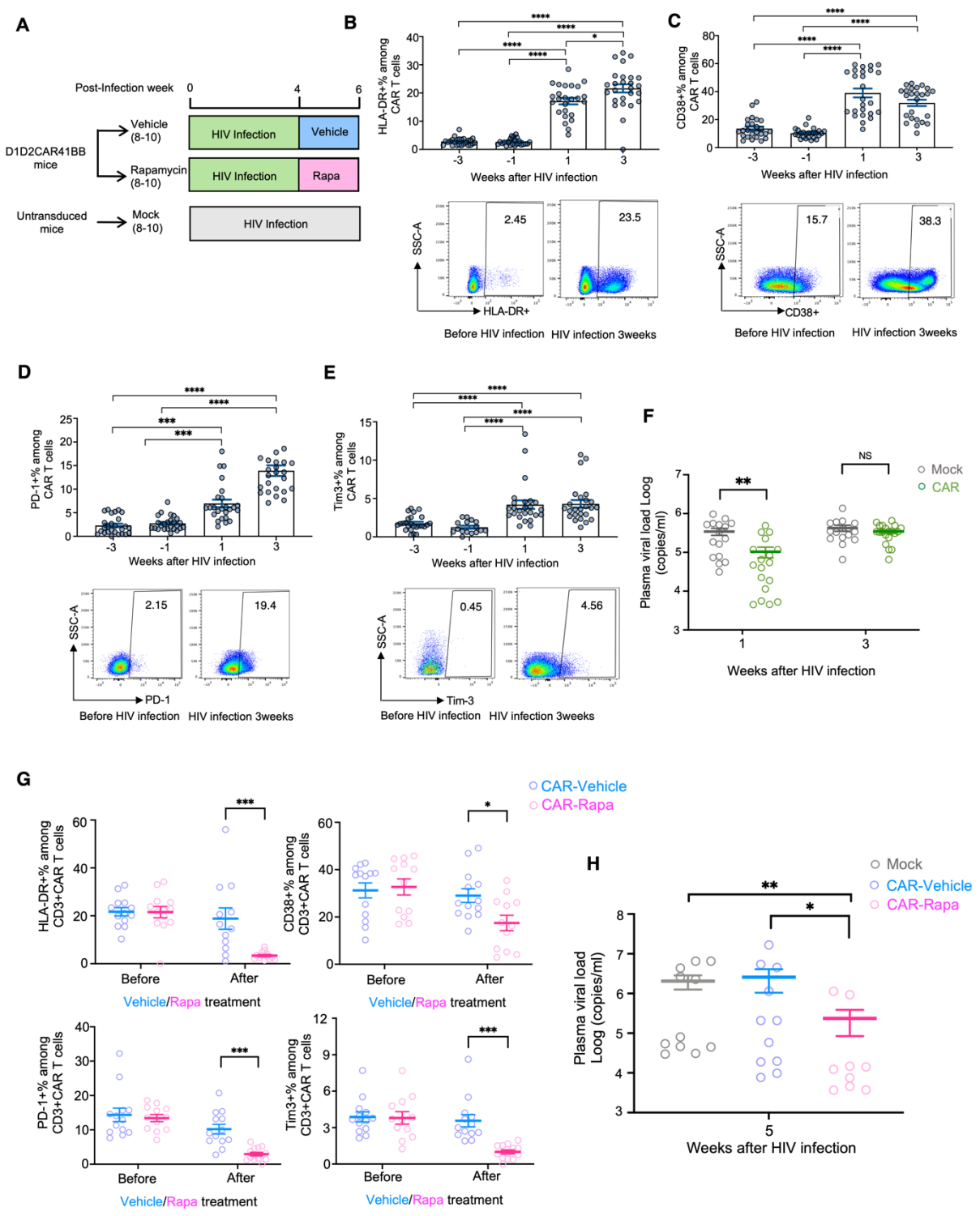
Figure 2 Chronic HIV infection leads to CAR-T cells exhaustion, while rapamycin treatment alleviates activation and exhaustion of CAR-T cells *in vivo*. A) Humanized NSG-BLT mice were constructed with either unmodified HSCs or HSCs modified with D1D2CAR41BB. After immune reconstitution, mice were infected with HIV-1$_{NFNSXL9}$. Four weeks after infection, mice with CAR modified HSCs were treated with rapamycin or vehicle for 2 weeks. (**B-E**) Representative flow and average percentage of B) HLA-DR, C) CD38, D) PD-1, E) Tim-3 expression among CAR+CD3+ T cells before and after HIV infection as measured by flow cytometry (quantified by gating of percentage positive ± SEM) (*n*=15-25 each group). (**F**) Plasma HIV viral load from mock or anti-HIV CAR mice at 1 week and 3 weeks of infection (*n*=15-18 each group). (**G**) Average percentage of PD-1, Tim3, HLA-DR and CD38 expression among blood CAR+CD3+ T cells before and after rapamycin treatment (*n*=10-15 each group). (**H**) Plasma HIV RNA copies from mock mice or CAR mice after 2 weeks of rapamycin or vehicle treatment (5 weeks after HIV infection) (*n*=9-11 each group). The Mann-Whitney test was used to compare 2 groups, and the Kruskal-Wallis test was used for multiple comparisons (**B-E**, and **H**); Each dot represents an individual mouse; horizontal bars indicate median values. *$P < 0.05$, **$P < 0.01$, ***$P < 0.001$, ****$P < 0.0001$.
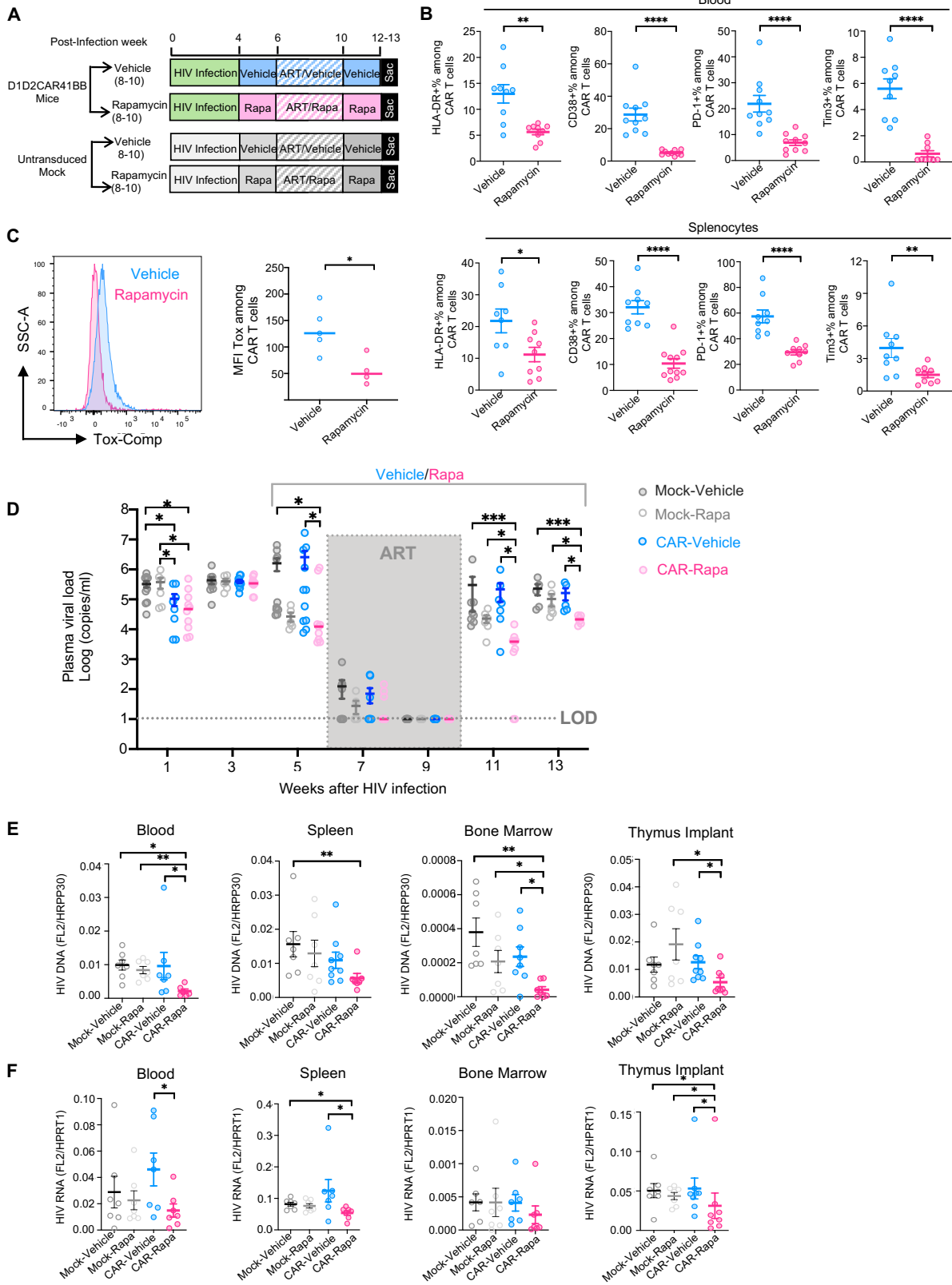
504
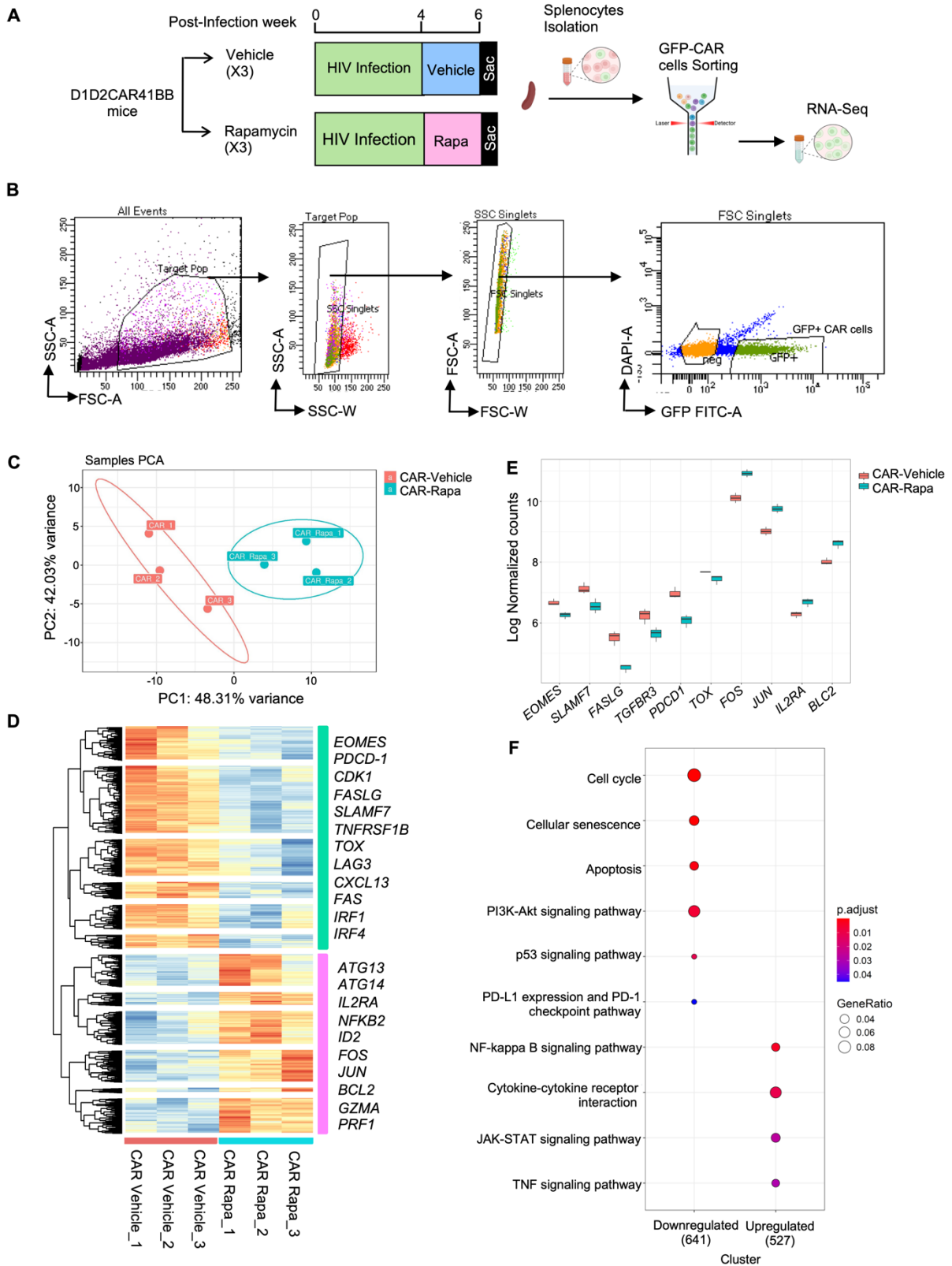
505 **Figure 3. Transcriptional signatures showed reduced exhaustion markers and upregulated of**

506 **memory and survival related signaling in CAR T cells in rapamycin treated mice. A)** Humanized NSG-

507 BLT mice with D1D2CAR41BB modified HSCs were treated with rapamycin or vehicle for 2 weeks before

508 necropsy. Afterwards, splenocytes were isolated and GFP+ CAR cells were sorted, and bulk RNA

509 sequencing was performed (*n*=3 per group). **B)** Representative flow cytometry analysis showing the gating

510 strategy for sorting of GFP+ CAR single cells. **C)** Principal component analysis and **D)** Heatmap showing

511 the relative expression (z score) of the top 5,000 genes that were differentially expressed between the 2

512 populations of CAR T cells derived from rapamycin-treated versus vehicle-treated CAR mice. Genes were

513 divided into downregulated (Green) and upregulated (Pink) clusters by K-means clustering based on

514 expression. **E)** Boxplot of Log normalized counts of genes important in T cell survival, activation, and

515 exhaustion. **F)** KEGG pathway analysis of differentially expressed genes among CAR T cells between

516 rapamycin-treated and vehicle-treated CAR mice. GeneRatio 'Gene ratio' is the percentage of total DEGs

517 in the given GO term.

518

519

520

521

A

Post-Infection week   0   4   6   10   12-13

D1D2CAR41BB Mice
→ Vehicle (8-10): HIV Infection | Vehicle | ART/Vehicle | Vehicle | Sac
→ Rapamycin (8-10): HIV Infection | Rapa | ART/Rapa | Rapa | Sac

Untransduced Mock
→ Vehicle 8-10): HIV Infection | Vehicle | ART/Vehicle | Vehicle | Sac
→ Rapamycin (8-10): HIV Infection | Rapa | ART/Rapa | Rapa | Sac

B Blood

HLA-DR+% among CAR T cells — Vehicle vs Rapamycin **
CD38+% among CAR T cells — Vehicle vs Rapamycin ****
PD-1+% among CAR T cells — Vehicle vs Rapamycin ****
Tim3+% among CAR T cells — Vehicle vs Rapamycin ****

C

SSC-A vs Tox-Comp — Vehicle / Rapamycin

Sample Name	Subset Name	Count
Spl_23.fcs	CAR	19520
Spl_3.fcs	CAR	3985

MFI Tox among CAR T cells — Vehicle vs Rapamycin

Splenocytes

HLA-DR+% among CAR T cells — Vehicle vs Rapamycin *
CD38+% among CAR T cells — Vehicle vs Rapamycin ****
PD-1+% among CAR T cells — Vehicle vs Rapamycin ****
Tim3+% among CAR T cells — Vehicle vs Rapamycin **

D

Vehicle/Rapa

Mock-Vehicle
Mock-Rapa
CAR-Vehicle
CAR-Rapa

Plasma viral load Loog (copies/ml) vs Weeks after HIV infection

ART   LOD

E

Blood — HIV DNA (FL2/HRPP30)
Spleen — HIV DNA (FL2/HRPP30)
Bone Marrow — HIV DNA (FL2/HRPP30)
Thymus Implant — HIV DNA (FL2/HRPP30)

Mock-Vehicle | Mock-Rapa | CAR-Vehicle | CAR-Rapa

F

Blood — HIV RNA (FL2/HPRT1)
Spleen — HIV RNA (FL2/HPRT1)
Bone Marrow — HIV RNA (FL2/HPRT1)
Thymus Implant — HIV RNA (FL2/HPRT1)

Mock-Vehicle | Mock-Rapa | CAR-Vehicle | CAR-Rapa

522

27

Figure 4: Long-term low dose rapamycin treatment in combination with ART alleviated CAR-T cell exhaustion and reduced viral rebound. A) Humanized NSG-BLT mice with either D1D2CAR41BB modified or non-modified HSCs were infected with HIV and treated with rapamycin or vehicle for 2 weeks. Afterwards, while continuing rapamycin or vehicle treatment, mice were treated with ART for 4 weeks, followed by ART interruption for 2-3 weeks. (**B**) PD-1, Tim-3, HLA-DR and CD38 expression was measured by flow cytometry (quantified by gating percentage positive cells) on peripheral blood(top) or spleen(bottom) CD3 CAR+T cells (*n*=8-10 per group). **C)** Splenocytes from CAR mice treated with ART and rapamycin or vehicle were isolated and stained with intracellular Abs against human Tox1. MFIs of the Tox1 on CAR+ T cells were measured by flow cytometry (*n*=5 per group). **D)** Longitudinal HIV viral load in plasma from humanized mice after rapamycin or vehicle treatment were measured by real-time PCR (*n*=4-7 per group). Dotted line indicates limit of detection. **E)** HIV DNA copies per cell from PBMC, splenocytes, bone marrow or thymus implant from different groups of mice as measured by real-time PCR. Human HRPP30 gene was used as internal control (*n*=7-9 per group). **F)** Relative HIV cellular RNA expression from multiple lymphoid tissues from different groups of mice as measured by real-time PCR. Human HPRT1 gene expression was used as internal control (*n*=7–8 per group). The Mann-Whitney test was used to compare 2 groups, and the Kruskal-Wallis test was used for multiple comparisons (**D, E and F**); *$P < 0.05$, **$P < 0.01$, ***$P < 0.001$, ****$P < 0.0001$.

542

29
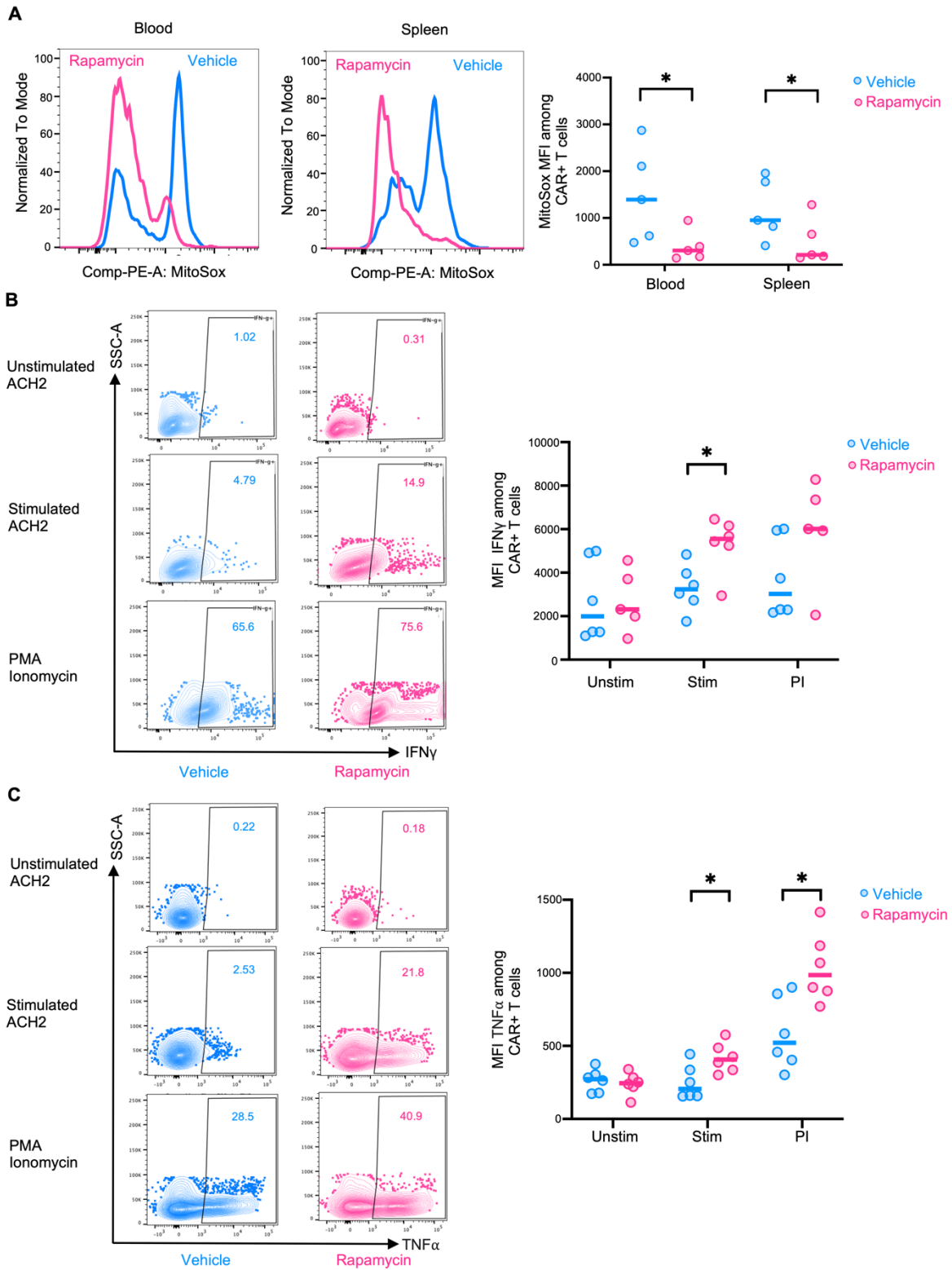
543   **Figure 5. Rapamycin treatment decreases mitochondria ROS and improves CAR T function *in vivo*.**

544   **A)** ROS levels analyzed by MitoSOX staining in blood or spleen CAR T cells isolated from CAR mice

545   treated with either rapamycin or vehicle (*n*=5 per group). **B-C)** Splenocytes from CAR transduced, HIV-

546   1–infected, vehicle-treated, or rapamycin-treated mice were stimulated with PMA/ionomycin, or envelope

547   expressing (stimulated ACH2) or non-expressing (unstimulated ACH2) cells and production of IFN-γ and

548   TNF-α by CAR T cells was measured by flow cytometry (*n*=5-6 per group). Representative flow cytometry

549   data showing percentage and MFI of IFN-γ^{+} **(B)** and TNF-α **(C)** among CAR T cells from HIV-1–infected,

550   vehicle-treated, or rapamycin-treated mice. Each dot represents an individual mouse; horizontal bars

551   indicate median values. Mann-Whitney test (unpaired); *$P < 0.05$, **$P < 0.01$.

552
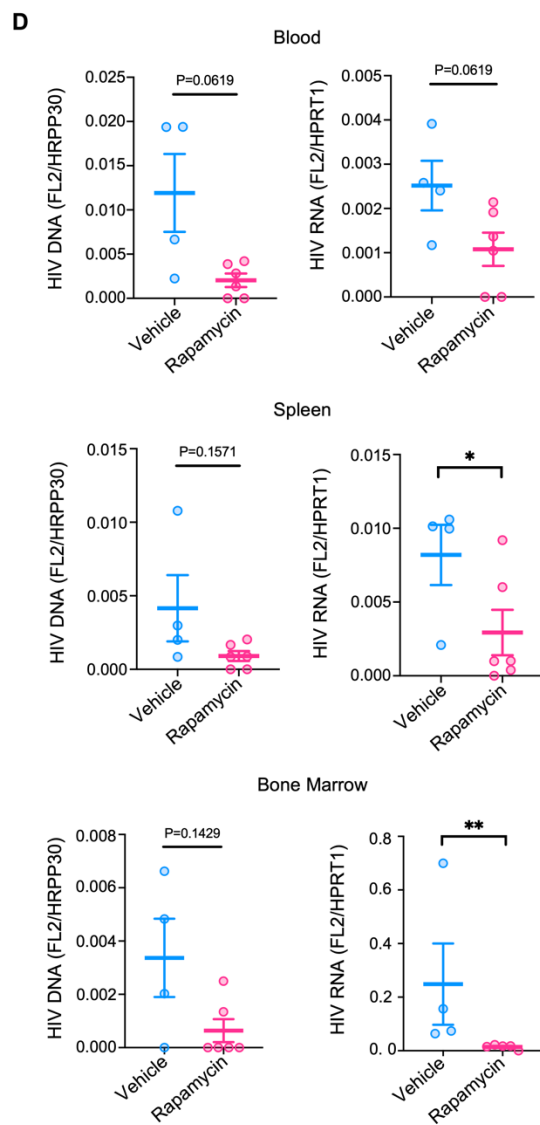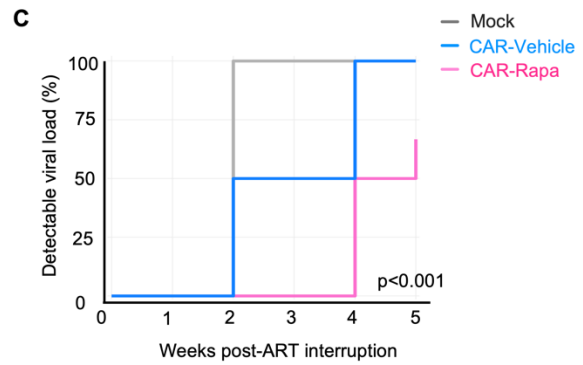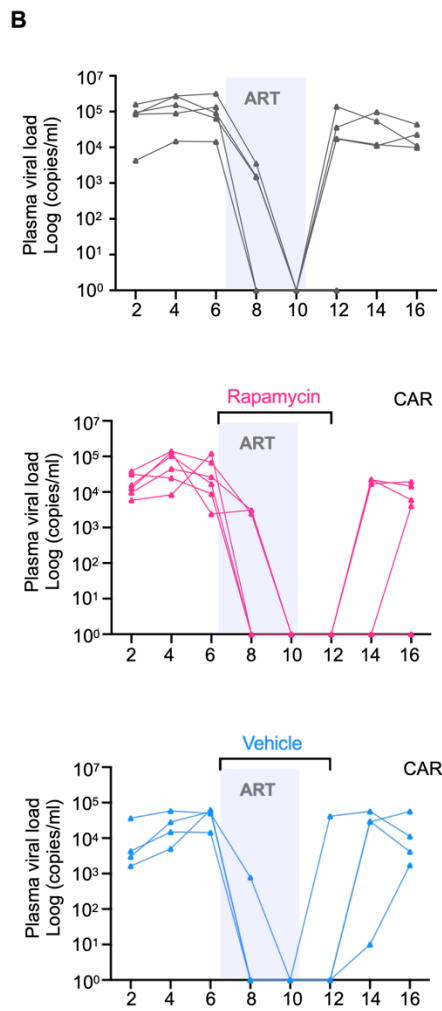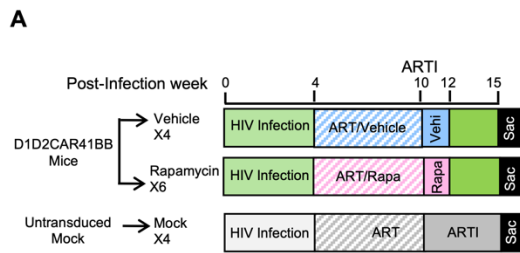
554 **Figure 6. Rapamycin treated NSG-IL-15 CAR mice showed significantly delayed viral rebound and**

555 **smaller reservoirs after ART withdraw. A)** Humanized NSG-IL15-BLT mice were constructed with

556 either unmodified HSCs or HSCs modified with D1D2CAR41BB. After immune reconstitution, mice were

557 infected with HIV-1$_{NFNSXL9}$. Four weeks after infection, mock mice were treated with ART only. Mice with

558 CAR modified HSCs were treated with rapamycin or vehicle along with ART. Following successful viral

559 load suppression, ART was interrupted, and rapamycin or vehicle treatment continued for two additional

560 week before discontinuation (*n*=4-6 per group). **B)** Longitudinal plasma HIV viral load as measured by

561 real-time PCR. Dotted line indicates limit of detection. **C)** Survival analysis of time to detectable viral load

562 among mock, CAR mice that were treated with vehicle or rapamycin. p<0.0001 by log-rank test. **D)** HIV

563 DNA and relative cellular HIV RNA expression from blood PBMCs, splenocytes and bone marrow as

564 measured by real-time PCR. Mann-Whitney test (unpaired); *P < 0.05, **P < 0.01.

565

566

567   **Supplemental Figure**
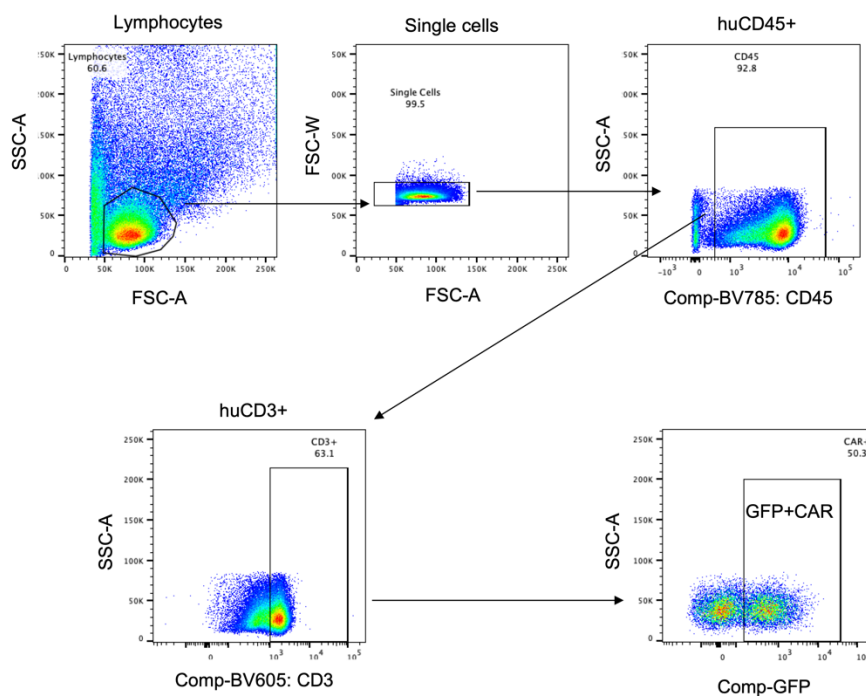
568

569   **SFig.1** Representative flow gating huCD45+CD3+GFP+CAR T by flow cytometry from peripheral blood.

570

571

572

573

574
575

References

577 1. Collins DR, Gaiha GD, and Walker BD. CD8(+) T cells in HIV control, cure and prevention. *Nat Rev*
578   *Immunol.* 2020;20(8):471-82.
579 2. Perdomo-Celis F, Taborda NA, and Rugeles MT. CD8(+) T-Cell Response to HIV Infection in the Era of
580   Antiretroviral Therapy. *Front Immunol.* 2019;10:1896.
581 3. Deng K, Pertea M, Rongvaux A, Wang L, Durand CM, Ghiaur G, et al. Broad CTL response is required to
582   clear latent HIV-1 due to dominance of escape mutations. *Nature.* 2015;517(7534):381-5.
583 4. Blackburn SD, Shin H, Haining WN, Zou T, Workman CJ, Polley A, et al. Coregulation of CD8+ T cell
584   exhaustion by multiple inhibitory receptors during chronic viral infection. *Nat Immunol.* 2009;10(1):29-37.
585 5. Marsden MD, and Zack JA. Double trouble: HIV latency and CTL escape. *Cell Host Microbe.*
586   2015;17(2):141-2.
587 6. Mu W, Carrillo MA, and Kitchen SG. Engineering CAR T Cells to Target the HIV Reservoir. *Front Cell*
588   *Infect Microbiol.* 2020;10:410.
589 7. Louie RHY, Kaczorowski KJ, Barton JP, Chakraborty AK, and McKay MR. Fitness landscape of the
590   human immunodeficiency virus envelope protein that is targeted by antibodies. *Proc Natl Acad Sci U S A.*
591   2018;115(4):E564-E73.
592 8. Yang OO, Tran AC, Kalams SA, Johnson RP, Roberts MR, and Walker BD. Lysis of HIV-1-infected cells
593   and inhibition of viral replication by universal receptor T cells. *Proc Natl Acad Sci U S A.*
594   1997;94(21):11478-83.
595 9. Rafiq S, Hackett CS, and Brentjens RJ. Engineering strategies to overcome the current roadblocks in CAR
596   T cell therapy. *Nat Rev Clin Oncol.* 2020;17(3):147-67.
597 10. Zhen A, Carrillo MA, Mu W, Rezek V, Martin H, Hamid P, et al. Robust CAR-T memory formation and
598   function via hematopoietic stem cell delivery. *PLoS pathogens.* 2021;17(4):e1009404.
599 11. Zhen A, Kamata M, Rezek V, Rick J, Levin B, Kasparian S, et al. HIV-specific Immunity Derived From
600   Chimeric Antigen Receptor-engineered Stem Cells. *Molecular therapy : the journal of the American*
601   *Society of Gene Therapy.* 2015;23(8):1358-67.
602 12. Zhen A, Peterson CW, Carrillo MA, Reddy SS, Youn CS, Lam BB, et al. Long-term persistence and
603   function of hematopoietic stem cell-derived chimeric antigen receptor T cells in a nonhuman primate model
604   of HIV/AIDS. *PLoS pathogens.* 2017;13(12):e1006753.
605 13. Carrillo MA, Zhen A, Mu W, Rezek V, Martin H, Peterson CW, et al. Stem cell-derived CAR T cells show
606   greater persistence, trafficking, and viral control compared to ex vivo transduced CAR T cells. *Molecular*
607   *therapy : the journal of the American Society of Gene Therapy.* 2024;32(4):1000-15.
608 14. Pauken KE, and Wherry EJ. Overcoming T cell exhaustion in infection and cancer. *Trends Immunol.*
609   2015;36(4):265-76.
610 15. Maldini CR, Claiborne DT, Okawa K, Chen T, Dopkin DL, Shan X, et al. Dual CD4-based CAR T cells
611   with distinct costimulatory domains mitigate HIV pathogenesis in vivo. *Nature medicine.*
612   2020;26(11):1776-87.
613 16. Rust BJ, Kean LS, Colonna L, Brandenstein KE, Poole NH, Obenza W, et al. Robust expansion of HIV
614   CAR T cells following antigen boosting in ART-suppressed nonhuman primates. *Blood.*
615   2020;136(15):1722-34.
616 17. Grosser R, Cherkassky L, Chintala N, and Adusumilli PS. Combination Immunotherapy with CAR T Cells
617   and Checkpoint Blockade for the Treatment of Solid Tumors. *Cancer Cell.* 2019;36(5):471-82.
618 18. Martins F, Sofiya L, Sykiotis GP, Lamine F, Maillard M, Fraga M, et al. Adverse effects of immune-
619   checkpoint inhibitors: epidemiology, management and surveillance. *Nat Rev Clin Oncol.* 2019;16(9):563-
620   80.
621 19. Bajwa R, Cheema A, Khan T, Amirpour A, Paul A, Chaughtai S, et al. Adverse Effects of Immune
622   Checkpoint Inhibitors (Programmed Death-1 Inhibitors and Cytotoxic T-Lymphocyte-Associated Protein-4
623   Inhibitors): Results of a Retrospective Study. *J Clin Med Res.* 2019;11(4):225-36.
624 20. Mannick JB, and Lamming DW. Targeting the biology of aging with mTOR inhibitors. *Nat Aging.*
625   2023;3(6):642-60.
626 21. Mannick JB, Del Giudice G, Lattanzi M, Valiante NM, Praestgaard J, Huang B, et al. mTOR inhibition
627   improves immune function in the elderly. *Science translational medicine.* 2014;6(268):268ra179.
628 22. Mannick JB, Teo G, Bernardo P, Quinn D, Russell K, Klickstein L, et al. Targeting the biology of ageing
629   with mTOR inhibitors to improve immune function in older adults: phase 2b and phase 3 randomised trials.
630   *Lancet Healthy Longev.* 2021;2(5):e250-e62.

631 23. Di Benedetto F, Di Sandro S, De Ruvo N, Montalti R, Ballarin R, Guerrini GP, et al. First report on a series
632   of HIV patients undergoing rapamycin monotherapy after liver transplantation. *Transplantation.*
633   2010;89(6):733-8.

634 24. Henrich TJ, Schreiner C, Cameron C, Hogan LE, Richardson B, Rutishauser RL, et al. Everolimus, an
635   mTORC1/2 inhibitor, in ART-suppressed individuals who received solid organ transplantation: A
636   prospective study. *Am J Transplant.* 2021;21(5):1765-79.

637 25. Wirth M, Schwarz C, Benson G, Horn N, Buchert R, Lange C, et al. Effects of spermidine supplementation
638   on cognition and biomarkers in older adults with subjective cognitive decline (SmartAge)-study protocol
639   for a randomized controlled trial. *Alzheimers Res Ther.* 2019;11(1):36.

640 26. Pollizzi KN, Patel CH, Sun IH, Oh MH, Waickman AT, Wen J, et al. mTORC1 and mTORC2 selectively
641   regulate CD8(+) T cell differentiation. *The Journal of clinical investigation.* 2015;125(5):2090-108.

642 27. Pearce EL, Walsh MC, Cejas PJ, Harms GM, Shen H, Wang LS, et al. Enhancing CD8 T-cell memory by
643   modulating fatty acid metabolism. *Nature.* 2009;460(7251):103-7.

644 28. Mannick JB, Morris M, Hockey HP, Roma G, Beibel M, Kulmatycki K, et al. TORC1 inhibition enhances
645   immune function and reduces infections in the elderly. *Science translational medicine.* 2018;10(449).

646 29. Ando S, Perkins CM, Sajiki Y, Chastain C, Valanparambil RM, Wieland A, et al. mTOR regulates T cell
647   exhaustion and PD-1-targeted immunotherapy response during chronic viral infection. *The Journal of*
648   *clinical investigation.* 2023;133(2).

649 30. Mu W, Rezek V, Martin H, Carrillo MA, Tomer S, Hamid P, et al. Autophagy inducer rapamycin treatment
650   reduces IFN-I-mediated Inflammation and improves anti-HIV-1 T cell response in vivo. *JCI insight.*
651   2022;7(22).

652 31. McLane LM, Abdel-Hakeem MS, and Wherry EJ. CD8 T Cell Exhaustion During Chronic Viral Infection
653   and Cancer. *Annu Rev Immunol.* 2019;37:457-95.

654 32. Hashimoto M, Kamphorst AO, Im SJ, Kissick HT, Pillai RN, Ramalingam SS, et al. CD8 T Cell
655   Exhaustion in Chronic Infection and Cancer: Opportunities for Interventions. *Annual review of medicine.*
656   2018;69:301-18.

657 33. Alfei F, Kanev K, Hofmann M, Wu M, Ghoneim HE, Roelli P, et al. TOX reinforces the phenotype and
658   longevity of exhausted T cells in chronic viral infection. *Nature.* 2019;571(7764):265-9.

659 34. Scott AC, Dundar F, Zumbo P, Chandran SS, Klebanoff CA, Shakiba M, et al. TOX is a critical regulator
660   of tumour-specific T cell differentiation. *Nature.* 2019;571(7764):270-4.

661 35. Khan O, Giles JR, McDonald S, Manne S, Ngiow SF, Patel KP, et al. TOX transcriptionally and
662   epigenetically programs CD8(+) T cell exhaustion. *Nature.* 2019;571(7764):211-8.

663 36. Buggert M, Tauriainen J, Yamamoto T, Frederiksen J, Ivarsson MA, Michaelsson J, et al. T-bet and Eomes
664   are differentially linked to the exhausted phenotype of CD8+ T cells in HIV infection. *PLoS pathogens.*
665   2014;10(7):e1004251.

666 37. O'Connell P, Hyslop S, Blake MK, Godbehere S, Amalfitano A, and Aldhamen YA. SLAMF7 Signaling
667   Reprograms T Cells toward Exhaustion in the Tumor Microenvironment. *Journal of immunology*
668   *(Baltimore, Md : 1950).* 2021;206(1):193-205.

669 38. Seo W, Jerin C, and Nishikawa H. Transcriptional regulatory network for the establishment of CD8(+) T
670   cell exhaustion. *Exp Mol Med.* 2021;53(2):202-9.

671 39. Tietscher S, Wagner J, Anzeneder T, Langwieder C, Rees M, Sobottka B, et al. A comprehensive single-
672   cell map of T cell exhaustion-associated immune environments in human breast cancer. *Nature*
673   *communications.* 2023;14(1):98.

674 40. Sumida TS, Dulberg S, Schupp JC, Lincoln MR, Stillwell HA, Axisa PP, et al. Type I interferon
675   transcriptional network regulates expression of coinhibitory receptors in human T cells. *Nat Immunol.*
676   2022;23(4):632-42.

677 41. Shao L, Hou W, Scharping NE, Vendetti FP, Srivastava R, Roy CN, et al. IRF1 Inhibits Antitumor
678   Immunity through the Upregulation of PD-L1 in the Tumor Cell. *Cancer immunology research.*
679   2019;7(8):1258-66.

680 42. Man K, Gabriel SS, Liao Y, Gloury R, Preston S, Henstridge DC, et al. Transcription Factor IRF4
681   Promotes CD8(+) T Cell Exhaustion and Limits the Development of Memory-like T Cells during Chronic
682   Infection. *Immunity.* 2017;47(6):1129-41 e5.

683 43. Seo H, Gonzalez-Avalos E, Zhang W, Ramchandani P, Yang C, Lio CJ, et al. BATF and IRF4 cooperate to
684   counter exhaustion in tumor-infiltrating CAR T cells. *Nat Immunol.* 2021;22(8):983-95.

685 44. Lynn RC, Weber EW, Sotillo E, Gennert D, Xu P, Good Z, et al. c-Jun overexpression in CAR T cells
686   induces exhaustion resistance. *Nature.* 2019;576(7786):293-300.

687 45. Karin M, Liu Z, and Zandi E. AP-1 function and regulation. *Curr Opin Cell Biol.* 1997;9(2):240-6.

688 46. Kim YC, and Guan KL. mTOR: a pharmacologic target for autophagy regulation. *The Journal of clinical*
689   *investigation.* 2015;125(1):25-32.

690 47. Yao C, Sun HW, Lacey NE, Ji Y, Moseman EA, Shih HY, et al. Single-cell RNA-seq reveals TOX as a key
691   regulator of CD8(+) T cell persistence in chronic infection. *Nat Immunol.* 2019;20(7):890-901.

692 48. Dickinson BC, and Chang CJ. Chemistry and biology of reactive oxygen species in signaling or stress
693   responses. *Nat Chem Biol.* 2011;7(8):504-11.

694 49. Finkel T, and Holbrook NJ. Oxidants, oxidative stress and the biology of ageing. *Nature.*
695   2000;408(6809):239-47.

696 50. Wu H, Zhao X, Hochrein SM, Eckstein M, Gubert GF, Knopper K, et al. Mitochondrial dysfunction
697   promotes the transition of precursor to terminally exhausted T cells through HIF-1alpha-mediated
698   glycolytic reprogramming. *Nature communications.* 2023;14(1):6858.

699 51. Peng HY, Lucavs J, Ballard D, Das JK, Kumar A, Wang L, et al. Metabolic Reprogramming and Reactive
700   Oxygen Species in T Cell Immunity. *Frontiers in immunology.* 2021;12:652687.

701 52. Yu YR, Imrichova H, Wang H, Chao T, Xiao Z, Gao M, et al. Disturbed mitochondrial dynamics in
702   CD8(+) TILs reinforce T cell exhaustion. *Nat Immunol.* 2020;21(12):1540-51.

703 53. Scharping NE, Menk AV, Moreci RS, Whetstone RD, Dadey RE, Watkins SC, et al. The Tumor
704   Microenvironment Represses T Cell Mitochondrial Biogenesis to Drive Intratumoral T Cell Metabolic
705   Insufficiency and Dysfunction. *Immunity.* 2016;45(2):374-88.

706 54. Bengsch B, Johnson AL, Kurachi M, Odorizzi PM, Pauken KE, Attanasio J, et al. Bioenergetic
707   Insufficiencies Due to Metabolic Alterations Regulated by the Inhibitory Receptor PD-1 Are an Early
708   Driver of CD8(+) T Cell Exhaustion. *Immunity.* 2016;45(2):358-73.

709 55. Abeynaike SA, Huynh TR, Mehmood A, Kim T, Frank K, Gao K, et al. Human Hematopoietic Stem Cell
710   Engrafted IL-15 Transgenic NSG Mice Support Robust NK Cell Responses and Sustained HIV-1 Infection.
711   *Viruses.* 2023;15(2).

712 56. Aryee KE, Burzenski LM, Yao LC, Keck JG, Greiner DL, Shultz LD, et al. Enhanced development of
713   functional human NK cells in NOD-scid-IL2rg(null) mice expressing human IL15. *FASEB journal :*
714   *official publication of the Federation of American Societies for Experimental Biology.* 2022;36(9):e22476.

715 57. June CH, O'Connor RS, Kawalekar OU, Ghassemi S, and Milone MC. CAR T cell immunotherapy for
716   human cancer. *Science.* 2018;359(6382):1361-5.

717 58. Deeks SG, Wagner B, Anton PA, Mitsuyasu RT, Scadden DT, Huang C, et al. A phase II randomized study
718   of HIV-specific T-cell gene therapy in subjects with undetectable plasma viremia on combination
719   antiretroviral therapy. *Mol Ther.* 2002;5(6):788-97.

720 59. Mitsuyasu RT, Anton PA, Deeks SG, Scadden DT, Connick E, Downs MT, et al. Prolonged survival and
721   tissue trafficking following adoptive transfer of CD4zeta gene-modified autologous CD4(+) and CD8(+) T
722   cells in human immunodeficiency virus-infected subjects. *Blood.* 2000;96(3):785-93.

723 60. Walker RE, Bechtel CM, Natarajan V, Baseler M, Hege KM, Metcalf JA, et al. Long-term in vivo survival
724   of receptor-modified syngeneic T cells in patients with human immunodeficiency virus infection. *Blood.*
725   2000;96(2):467-74.

726 61. Beauparlant D, Rusert P, Magnus C, Kadelka C, Weber J, Uhr T, et al. Delineating CD4 dependency of
727   HIV-1: Adaptation to infect low level CD4 expressing target cells widens cellular tropism but severely
728   impacts on envelope functionality. *PLoS Pathog.* 2017;13(3):e1006255.

729 62. Leibman RS, Richardson MW, Ellebrecht CT, Maldini CR, Glover JA, Secreto AJ, et al. Supraphysiologic
730   control over HIV-1 replication mediated by CD8 T cells expressing a re-engineered CD4-based chimeric
731   antigen receptor. *PLoS pathogens.* 2017;13(10):e1006613.

732 63. Anthony-Gonda K, Ray A, Su H, Wang Y, Xiong Y, Lee D, et al. In vivo killing of primary HIV-infected
733   cells by peripheral-injected early memory-enriched anti-HIV duoCAR T cells. *JCI insight.* 2022;7(21).

734 64. Anthony-Gonda K, Bardhi A, Ray A, Flerin N, Li M, Chen W, et al. Multispecific anti-HIV duoCAR-T
735   cells display broad in vitro antiviral activity and potent in vivo elimination of HIV-infected cells in a
736   humanized mouse model. *Science translational medicine.* 2019;11(504).

737 65. Barber-Axthelm IM, Barber-Axthelm V, Sze KY, Zhen A, Suryawanshi GW, Chen IS, et al. Stem cell-
738   derived CAR T cells traffic to HIV reservoirs in macaques. *JCI insight.* 2021;6(1).

739 66. Carrillo MA, Zhen A, Zack JA, and Kitchen SG. New approaches for the enhancement of chimeric antigen
740   receptors for the treatment of HIV. *Transl Res.* 2017;187:83-92.

741 67. Zhen A, Carrillo MA, and Kitchen SG. Chimeric antigen receptor engineered stem cells: a novel HIV
742   therapy. *Immunotherapy.* 2017;9(5):401-10.

743 68. Zhen A, Rezek V, Youn C, Rick J, Lam B, Chang N, et al. Stem-cell Based Engineered Immunity Against
744   HIV Infection in the Humanized Mouse Model. *Journal of visualized experiments : JoVE.* 2016(113).
745 69. Mu W, Patankar V, Kitchen S, and Zhen A. Examining Chronic Inflammation, Immune Metabolism, and T
746   Cell Dysfunction in HIV Infection. *Viruses.* 2024;16(2).
747 70. Fenwick C, Joo V, Jacquier P, Noto A, Banga R, Perreau M, et al. T-cell exhaustion in HIV infection.
748   *Immunological reviews.* 2019;292(1):149-63.
749 71. Zhen A, Rezek V, Youn C, Lam B, Chang N, Rick J, et al. Targeting type I interferon-mediated activation
750   restores immune function in chronic HIV infection. *The Journal of clinical investigation.* 2017;127(1):260-
751   8.
752 72. Mu W, Martin H, and Zhen A. Targeting autophagy to treat HIV immune dysfunction. *Autophagy Rep.*
753   2023;2(1).
754 73. Lee DJW, Hodzic Kuerec A, and Maier AB. Targeting ageing with rapamycin and its derivatives in
755   humans: a systematic review. *Lancet Healthy Longev.* 2024;5(2):e152-e62.
756 74. Rodes B, Cadinanos J, Esteban-Cantos A, Rodriguez-Centeno J, and Arribas JR. Ageing with HIV:
757   Challenges and biomarkers. *EBioMedicine.* 2022;77:103896.
758 75. Babu H, Ambikan AT, Gabriel EE, Svensson Akusjarvi S, Palaniappan AN, Sundaraj V, et al. Systemic
759   Inflammation and the Increased Risk of Inflamm-Aging and Age-Associated Diseases in People Living
760   With HIV on Long Term Suppressive Antiretroviral Therapy. *Frontiers in immunology.* 2019;10:1965.
761 76. Nasi M, De Biasi S, Gibellini L, Bianchini E, Pecorini S, Bacca V, et al. Ageing and inflammation in
762   patients with HIV infection. *Clin Exp Immunol.* 2017;187(1):44-52.
763 77. Henrich TJ, Bosch RJ, Godfrey C, Mar H, Nair A, Keefer M, et al. Sirolimus reduces T cell cycling,
764   immune checkpoint marker expression, and HIV-1 DNA in people with HIV. *Cell Rep Med.*
765   2024;5(10):101745.
766 78. Stock PG, Barin B, Hatano H, Rogers RL, Roland ME, Lee TH, et al. Reduction of HIV persistence
767   following transplantation in HIV-infected kidney transplant recipients. *Am J Transplant.* 2014;14(5):1136-
768   41.
769 79. Besnard E, Hakre S, Kampmann M, Lim HW, Hosmane NN, Martin A, et al. The mTOR Complex
770   Controls HIV Latency. *Cell Host Microbe.* 2016;20(6):785-97.
771 80. Araki K, Turner AP, Shaffer VO, Gangappa S, Keller SA, Bachmann MF, et al. mTOR regulates memory
772   CD8 T-cell differentiation. *Nature.* 2009;460(7251):108-12.
773 81. Chi H. Regulation and function of mTOR signalling in T cell fate decisions. *Nature reviews Immunology.*
774   2012;12(5):325-38.
775 82. Varco-Merth BD, Brantley W, Marenco A, Duell DD, Fachko DN, Richardson B, et al. Rapamycin limits
776   CD4+ T cell proliferation in simian immunodeficiency virus-infected rhesus macaques on antiretroviral
777   therapy. *The Journal of clinical investigation.* 2022;132(10).
778 83. Kouro T, Himuro H, and Sasada T. Exhaustion of CAR T cells: potential causes and solutions. *Journal of
779   translational medicine.* 2022;20(1):239.
780 84. Mu W, Zhen A, Carrillo MA, Rezek V, Martin H, Lizarraga M, et al. Oral Combinational Antiretroviral
781   Treatment in HIV-1 Infected Humanized Mice. *Journal of visualized experiments : JoVE.* 2022(188).
782